A condensed approach to modeling and analysis of ferroelectrics

*Stephan Lange[1] and Andreas Ricoeur[2]

[1,2] *University of Kassel, Institute of Mechanics, 34125 Kassel, Germany*
[1] *stephan.lange@uni-kassel.de*

ABSTRACT

Ferroelectric, ferromagnetic or multiferroic materials as components of smart structures are widely used e.g. in aerospace or automotive technology. Although the material behavior of smart structures has been intensively studied during the past two decades there are still many open questions.

In this paper we present a micromechanically and physically motivated nonlinear constitutive model of ferroelectric materials. In contrast to most of the investigations on this topic, results for constitutive behavior are modeled without solving specific boundary value problems based on expensive FEM calculations. In fact, a simple numerical procedure is developed, on the one hand condensing the problem to a single material point or RVE, on the other maintaining features such as multiple grain interactions. Some results are presented and discussed in terms of hysteresis loops and residual stresses in a polycrystalline material.

1. INTRODUCTION

Ferroelectrics, as components of smart materials, are piezoelectric materials with the ability to switch their polarization direction under an applied mechanical (ferroelastic effect) or electric (ferroelectric effect) field. In the past two decades many researchers investigated the material behavior of smart structures (Huber et. al. (1999), Kamlah (2000, Enderlein (2007)). So, the material behavior of ferroelectrics in principle is well known. For the sake of analysis, ferroelectric structures are usually numerically simulated by the Finite Element (FE) method. The numerical results are commonly validated by experimental results, predominantly looking at different types of hysteresis loops (e.g. Hwang (1994)). At that point it is important to mention that the experimental results are usually based on a uniaxial loading. Within that context, it is dispensable to solve complex boundary value problems and thus a FE – implementation is redundant. In fact, it seems reasonable that the numerical simulation is decreased to an uniaxial problem without applying complex arithmetic techniques of a CAE software. However, grain-grain-interaction is crucial and taken into account still requiring a multi-dimensional tensorial mathematical framework for the constitutive model.

---

[1] PhD student
[2] Professor

In our approach polarization crosses replace the single grains of a representative volume element (RVE). Each polarization cross exhibits four perpendicular domain orientations and stands for one specific grain. In contrast to a FE approach, where grains are spatially distributed and commonly represented by Gaussian points, in the condensed model all material points, i.e. polarization crosses are concentrated in one spatial point. According to the domain structure of each point, these crosses can be arbitrarily oriented relative to the axis of the uniaxial boundary value problem. The resulting residual stresses between the grains due to the switching phenomena are realized by averaging within the framework of a Voigt approximation accounting for global equilibrium. First, we simulate the switching behavior of a single grain with an arbitrarily orientation. In the next step an arbitrary number of grains is realized but without residual stresses. Finally, residual stresses between the grains of the representative volume element are modeled by the above mentioned averaging technique.

2. THEORETICAL BACKGROUND

In the following, we present the governing field and constitutive equations for ferroelectric materials, the switching criterion and resultant Voigt approximation for our approach.

2.1 Governing field and constitutive equations

In ferroelectric materials, the domain wall motion leads to irreversible strain and polarization. Referring to the nonlinear effects of ferroelectric materials, many researchers investigated the material behavior in the past decades (e.g. Hwang et. al. (1994), Huber et. al. (1999), Kessler et. al. (2001), Enderlein (2007)). Therefore, we only show the resulting equations without any derivation.

The balance equations for mechanical and electrostatic equilibrium are

$$S_{ij,j} + b_i = 0,$$
$$D_{i,i} = w_V, \tag{1}$$

where volume forces and charges b_i and w_V are neglected in the following. Within the context of an uniaxial boundary value problem, only the x_1-coordinate is considered leading to the conditions

$$\frac{\partial S_{11}}{\partial x_1} = 0 \qquad \triangleright \qquad S_{11} = \text{const},$$
$$\frac{\partial D_1}{\partial x_1} = 0 \qquad \triangleright \qquad D_1 = \text{const}. \tag{2}$$

Stresses and electric displacements S_{22}, D_2 only occur, if there is a kinematic constraint

in the x_2-direction (uniaxial strain assumption).

The constitutive law for stress S_{ij} and electric displacement D_i of nonlinear ferroelectric material is shown in the following equations:

$$S_{ij} = C_{ijkl}\left(e_{kl}^{tot} - e_{kl}^{sp}\right) - e_{lij}E_l,$$
$$D_i = e_{ikl}\left(e_{kl}^{tot} - e_{kl}^{sp}\right) + \kappa_{il}E_l + P_i^{sp}. \tag{3}$$

In Eq. (3), C_{ijkl} describes the elastic, e_{lij} the piezoelectric and κ_{il} the dielectric constants of the given boundary problem. Further, $e_{kl}^{tot} - e_{kl}^{sp}$ stands for the recoverable strain as difference of total and spontaneous strains, E_l represents the electric field and P_i^{sp} describes the remanent polarization.

Due to tetragonal unit cells, the domain structure of a grain exhibits 90° and 180° domain walls. So, we have four polarization directions in each grain. Relating to a global coordinate system, the orientation of a grain is described by the angle φ. The volume fraction for each polarization direction is described by $v^{(N)}$. From that point, the following equations are valid for all grains.

$$0 \le v^{(n)} \le 1, \qquad \sum_{n=1}^{4} v^{(n)} = 1 \;, \quad \triangleright \quad v_0^{(n)} = \frac{1}{4} \;. \tag{4}$$

Here, $v_0^{(N)}$ describes the initial condition of volume fraction for each polarization direction. As a result of Eq. (4), the resulting material constants for a grain are

$$C_{ijkl} = \sum_{n=1}^{4} C_{ijkl}^{(n)}, \qquad e_{lij} = \sum_{n=1}^{4} e_{lij}^{(n)}, \qquad \kappa_{ij} = \sum_{n=1}^{4} \kappa_{ij}^{(n)}. \tag{5}$$

A variation of the volume fraction $v^{(N)}$ of domain N is equal to a domain wall motion. The domain wall motion is the result of switching processes of elementary cells and leads to a change of spontaneous polarization P_i^{sp}. Additionally, 90° switching processes yield a remanent strain e_{kl}^{sp}. These two quantities are shown in the resultant equations (Enderlein (2007)):

$$P_i^{sp} = bP^0 \begin{bmatrix} \sin\left(\varphi + \frac{1}{2}\beta\right) \\ -\cos\left(\varphi + \frac{1}{2}\beta\right) \end{bmatrix}, \qquad b = \begin{cases} \mp\sqrt{2} \;, & \beta = \pm 90° \\ -2 \;, & \beta = 180° \end{cases}, \qquad \varepsilon_{kl}^{sp} = \varepsilon_D \begin{bmatrix} \cos 2\varphi & \sin 2\varphi \\ \sin 2\varphi & -\cos 2\varphi \end{bmatrix} \cdot \tag{6}$$

In Eq. (6), b represents the switching direction and e_D is a temperature-dependent material parameter based on the lattice constants of a tetragonal elementary cell.

2.2 Switching criterion

The switching criterion for ferroelectric materials is well investigated and we only show the conclusion. For more detailed information look at Hwang (1994), Huber et. al. (1999) and Enderlein (2007). The simplified switching criterion, which is used in this paper, is given as

$$w_{diss} = S_{ij} e_{ij}^{sp} + E_i \mathrm{D} P_i^{sp} \geq w_{crit} = \left\{ \begin{array}{ll} 2P^0 E_C, & b=180° \\ \sqrt{2} P^0 E_C, & b=\pm 90° \end{array} \right. . \tag{7}$$

Here, e_{ij}^{sp} and $\mathrm{D}P_i^{sp}$ represent the switching strain and polarization of a domain species. These quantities are given in Eq. (6). E_C and P^0 are material properties and describe the coercive field strength and the lattice immanent polarization.

2.3 Averaging technique and Voigt approximation for representative volume element

In this section we want to focus on the Voigt approximation for the representative volume element. The idea of the presented method is motivated in the first paragraph. Here, all polarization crosses are combined in one point. The correlation between the grains is realized by a Voigt approximation. So, the macroscopic stress and strain of a macroscopic point is a volume average (Gross et. al. (2007))

$$\left\langle S_{ij} \right\rangle = \frac{1}{V} \int_V S_{ij}(x_l) dV \quad , \quad \left\langle e_{kl} \right\rangle = \frac{1}{V} \int_V e_{kl}(x_i) dV . \tag{8}$$

Eq. (8) shows the volume average for the macroscopic stress and strain. So, the macroscopic reversible strain is the result of the first constitutive law in Eq. (3):

$$\left\langle e_{kl}^{tot} - e_{kl}^{sp} \right\rangle = \left\langle C_{ijkl} \right\rangle^{-1} \left(\left\langle S_{ij} \right\rangle + \left\langle e_{lij} \right\rangle \left\langle E_l \right\rangle \right). \tag{9}$$

Here, $\left\langle C_{ijkl} \right\rangle, \left\langle e_{lij} \right\rangle$ and $\left\langle E_l \right\rangle$ are the volume averages of the microscopic quantities. For a discrete number of grains $k=1,\square ,M$ the volume integration is replaced by a summation. The averages of the material constants thus are given as

$$\left\langle C_{ijkl} \right\rangle = \frac{1}{M} \sum_{k=1}^{M} C_{ijkl}^{(k)} \quad , \quad \left\langle e_{lij} \right\rangle = \frac{1}{M} \sum_{k=1}^{M} e_{lij}^{(k)} \quad , \quad \left\langle \kappa_{ij} \right\rangle = \frac{1}{M} \sum_{k=1}^{M} \kappa_{ij}^{(k)} \quad . \tag{10}$$

Likewise, the electric field in Eq. (9) is averaged according to

$$\left\langle E_l \right\rangle = \frac{1}{M} \sum_{k=1}^{M} E_l^{(k)}. \tag{11}$$

Following a generalized Voigt approximation, the electric field is assumed to be constant in each grain. So, $\left\langle E_l \right\rangle$ is equal to E_l. The interpretation of Eq. (9) leads to the fact, that we have a constant state of strain in every grain k. Eq. (9) in association with Eq. (3) gives us the residual stress of grain k:

$$S_{ij}^{(k)} = C_{ijkl}^{(k)} \left\langle e_{kl}^{tot} - e_{kl}^{sp} \right\rangle - e_{lij}^{(k)} E_l. \tag{12}$$

Eq. (12), in connection with Eq. (7), yields the dissipative energy of grain k. Eqs. (9) and (12) provoke an interaction between the grains due to the switching induced residual stresses. An iterative procedure is required seeking an equilibrium for the domain configuration under external and residual loads.

3. NUMERICAL INVESTIGATION AND DISCUSSION

This paragraph deals with the numerical simulation of switching phenomena based on the model outlined above. At first we show the results of electric displacement D_i, total strain e_{kl}^{tot} and stress S_{ij} for a single grain. Here, we focus on different boundary conditions and their influence on the dissipative energy in Eq. (7). Then, we present the results for a polycrystalline system with arbitrarily orientations but without any interactions. Finally, we highlight some results of numerical investigations accounting for grain interaction. The material, which is modeled in this paragraph, is barium titanate ($BaTiO_3$). The applied material constants shown in the appendix.

3.1 Boundary conditions

For the numerical investigation we consider two boundary conditions (Fig. 1). Generally, the uniaxial strain assumption is applied. The first boundary condition *(a)* is a free rod (left sketch in Fig. 1). Our second boundary condition *(b)* is a clamped rod (right sketch in Fig. 1).
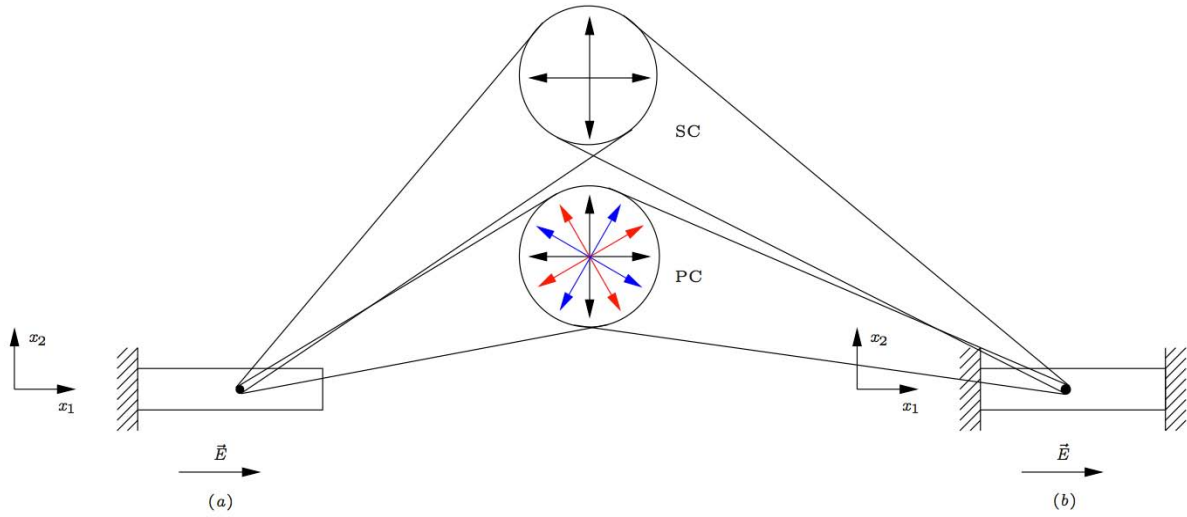
Fig. 1 Boundary conditions, single crystal (SC) and polycrystalline (PC) models

So, there are two different variants to determine the reversible strain which are shown in the following equations:

$$(a) \qquad S_{11} = 0 \qquad \triangleright \qquad e_{kl}^{tot} - e_{kl}^{sp} = e_{kl}^{rev} = C_{ijkl}^{-1} e_{lij} E_l$$

$$(13)$$

$$(b) \qquad e_{kl}^{tot} = 0 \qquad \triangleright \qquad e_{kl}^{rev} = -e_{kl}^{sp}$$

The applied electric field is a piecewise-linear function. All simulations start with an unpoled material, i.e. $v_0^{(n)} = 0,25$ for $n = 1, \square\ , 4$.

3.2 Numerical simulation for a single grain

In the following section we present the results of the numerical simulation for a single grain with boundary conditions *(a)* and *(b)*. The polarization cross is aligned with the global coordinate system, see Fig. 1.
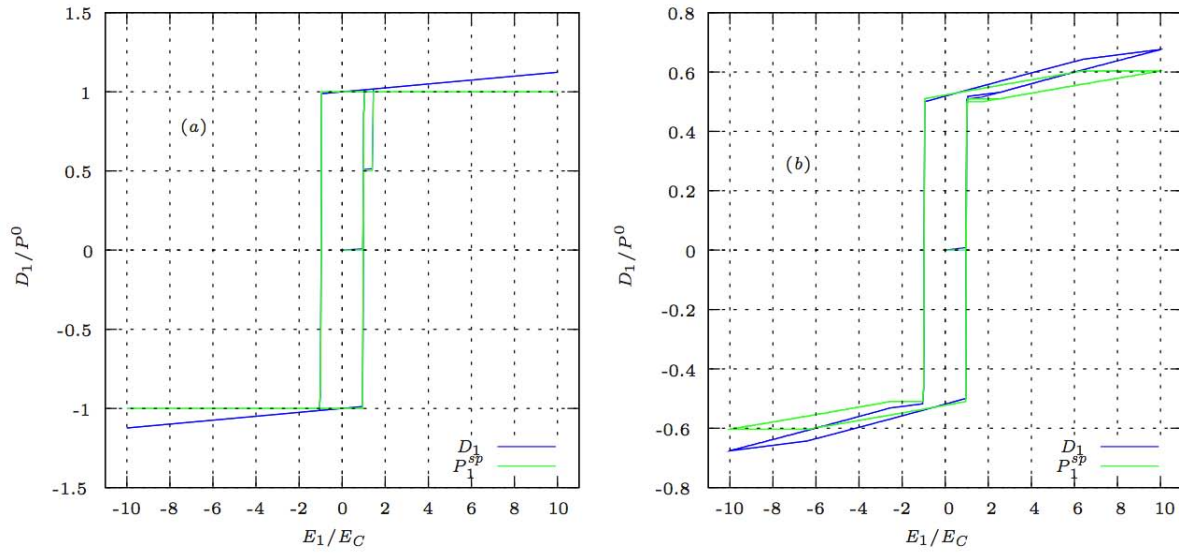
Fig. 2 Electric displacement vs. electric field for boundary conditions *(a)* and *(b)*

Fig. 2 shows the x_1-coordinate of electric displacement and remanent polarization vs. electric field for the boundary conditions *(a)* and *(b)*. First, we look at the results of boundary condition *(a)*. It is obvious that domains switch at $E_1 = E_C$ and $E_1 = \sqrt{2}E_C$. These electric fields are consistent with Eq. (7) taking into account boundary condition *(a)*. Because of the given boundary condition we have a full polarization in x_1-direction.

Looking at the results of boundary condition *(b)* we can see that the domains in negative x_1-direction switch at $E_1 = E_C$. This behavior is also consistent with Eq. (5) and equal to the behavior of boundary condition *(a)*. In contrast to boundary condition *(a)*, the domains in x_2-direction do not switch completely because of the resulting stresses, see Eq. (1), (5) and (10). The resulting stresses stop the switching process. So, it is necessary to increase the electric field and check the switching criteria again. Further, we can see that the domains in x_2-direction switch back into their initial position when the electric field is reduced. The same behavior of electric displacement and remanent polarization is observed for a negative electric field.

In Fig. 3 the results for total strain and stress vs. electric field are presented to confirm the results just discussed.

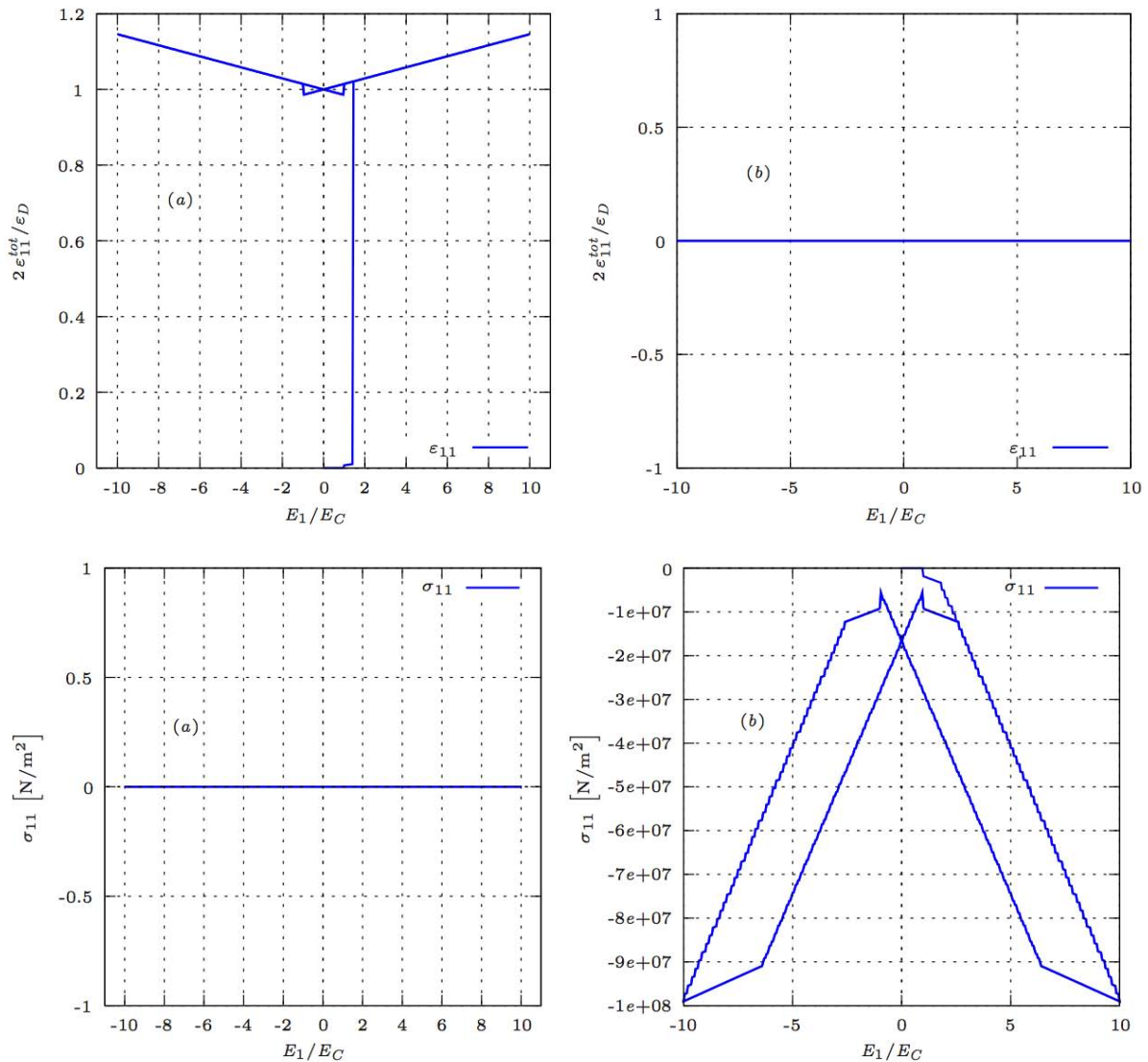Fig. 3 Total strain and stress vs. electric field for boundary conditions *(a)* and *(b)*

3.3 Numerical simulation for polycrystal without grain interaction

In this section we present the results for grains without interaction. Here, five grains with different orientation are considered. For this simulation, only boundary condition *(a)* is investigated. In the past section, boundary condition *(b)* has been established to show the influence of stresses in conjunction with 90° switching processes. With respect to the interaction of grains a similar behavior is expected, however now due to residual stresses.
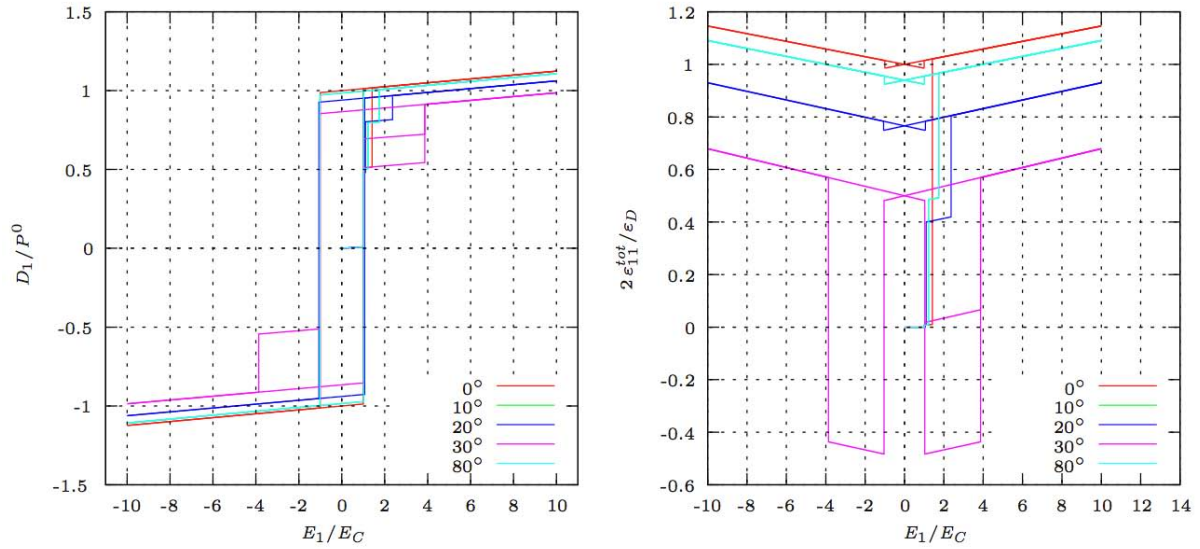
Fig. 4 Electric displacement and strain vs. electric field for different grains

Fig. 4 presents the results of the numerical simulation with five differently orientated polarizations crosses. In general, the orientations are random. Due to the limited number, the angles have been chosen explicitly. The presented results are reasonable and are in accordance with the dissipative energy in Eq. (5).

3.4 Residual stresses due to grain interaction

The last part of this paragraph deals with the numerical simulation of residual stresses. These are essential for the macroscopic constitutive behavior. Together with external loads they control domain wall motion and are responsible for the smoothness of hysteresis loops as observed in experiments. Although the boundary condition and balance equations imply an uniaxial field problem, residual stresses are those of a plane problem, i.e. S_{11}, S_{12} and S_{22} are non-zero.

Now, ten grains with arbitrary angles are considered. For this numerical simulation we have chosen boundary condition (a). That means, that $\langle S_{ij} \rangle$ in Eq. (9) is equal to zero. In Fig. 5 the results for residual $S_{ij}^{(k)}$ and average stresses $\langle S_{ij} \rangle$ are presented. The latter have been calculated from all $S_{ij}^{(k)}$ for verification.

stress component σ_{11}
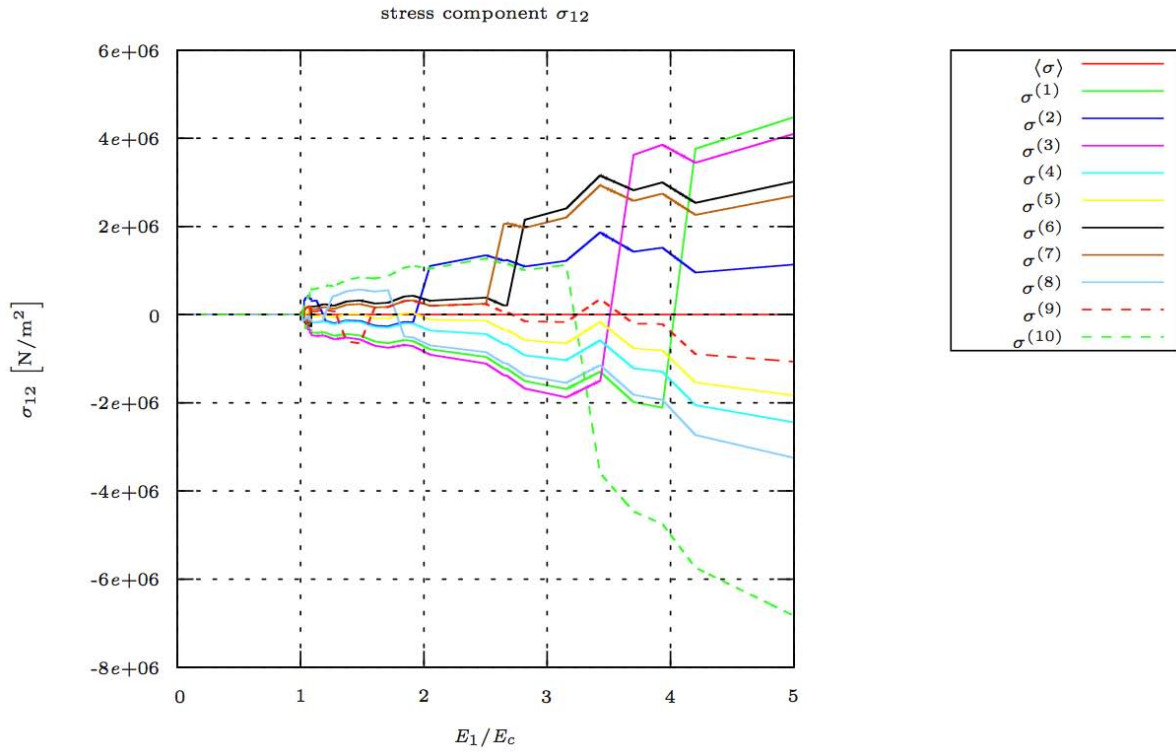

stress component σ_{22}
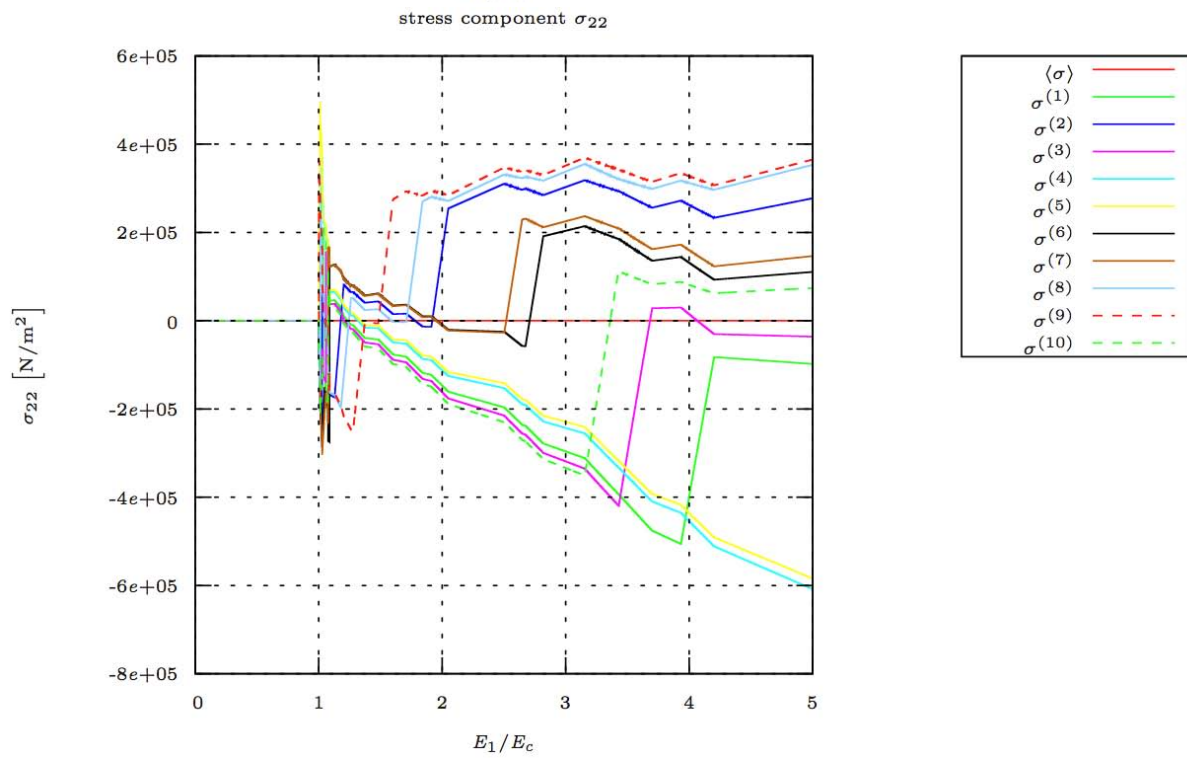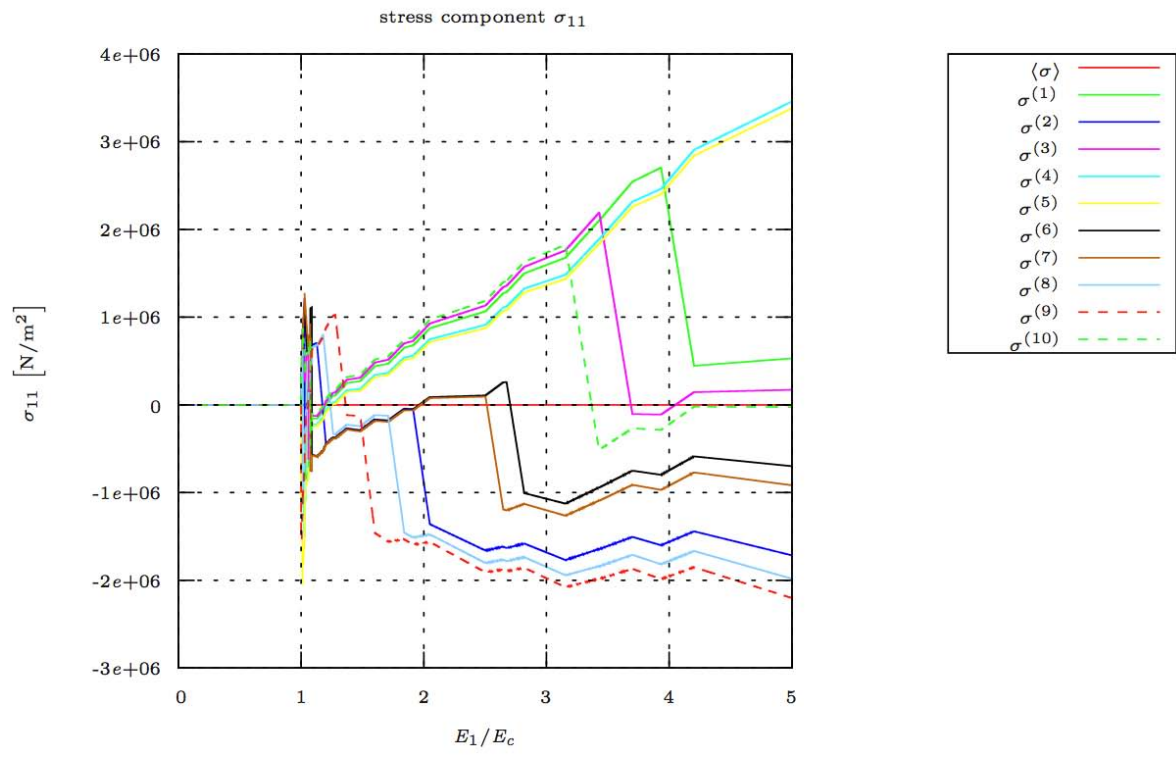
Fig. 5 Residual stress components vs. electric field for ten grains in a polycrystalline ferroelectric

Looking at the components of the stress tensor, it is obvious that some grains exhibit a positive (tensile) and some a negative (compression) residual stress. The average stress $\langle S_{ij} \rangle$ however, which is defined by

$$\langle S_{ij} \rangle = \frac{1}{M} \overset{M}{\underset{k=1}{\mathring{a}}} S_{ij}^{(k)},$$

(14)

is equal to zero for each component of the stress tensor. This behavior agrees with our chosen boundary condition.

4. CLOSURE

The goal of this paper was to present a micromechanically and physically motivated nonlinear constitutive model for ferroelectric materials in connection with an approach, which can simulate the material behavior without having to apply a discretization scheme. The method is applied to single grains as well as polycrystalline systems.

5. APPENDIX

Transversal isotropy with poling into the positive x_1-direction:

$$
C_{pq} = \begin{bmatrix}
C_{33} & C_{13} & C_{13} & 0 & 0 & 0 \\
C_{13} & C_{11} & C_{12} & 0 & 0 & 0 \\
C_{13} & C_{12} & C_{11} & 0 & 0 & 0 \\
0 & 0 & 0 & \dfrac{C_{11} - C_{12}}{2} & 0 & 0 \\
0 & 0 & 0 & 0 & C_{44} & 0 \\
0 & 0 & 0 & 0 & 0 & C_{44}
\end{bmatrix},
$$

$$
e_{kp} = \begin{bmatrix}
e_{33} & e_{31} & e_{31} & 0 & 0 & 0 \\
0 & 0 & 0 & 0 & 0 & e_{15} \\
0 & 0 & 0 & 0 & e_{15} & 0
\end{bmatrix},
$$

$$
k_{ij} = \begin{bmatrix}
k_{33} & 0 & 0 \\
0 & k_{11} & 0 \\
0 & 0 & k_{11}
\end{bmatrix}.
$$

Transversal isotropy with poling into the positive x_2-direction:

$$
C_{pq} = \begin{bmatrix}
C_{11} & C_{13} & C_{12} & 0 & 0 & 0 \\
C_{13} & C_{33} & C_{13} & 0 & 0 & 0 \\
C_{12} & C_{13} & C_{11} & 0 & 0 & 0 \\
0 & 0 & 0 & C_{44} & 0 & 0 \\
0 & 0 & 0 & 0 & \dfrac{C_{11} - C_{12}}{2} & 0 \\
0 & 0 & 0 & 0 & 0 & C_{44}
\end{bmatrix},
$$

$$
e_{kp} = \begin{bmatrix}
0 & 0 & 0 & 0 & 0 & e_{15} \\
e_{31} & e_{33} & e_{31} & 0 & 0 & 0 \\
0 & 0 & 0 & e_{15} & 0 & 0
\end{bmatrix},
$$

$$
k_{ij} = \begin{bmatrix}
k_{11} & 0 & 0 \\
0 & k_{33} & 0 \\
0 & 0 & k_{11}
\end{bmatrix}.
$$

Material constants and other used parameters of barium titanate (Jaffe et. al. (1971)):

$$C_{11} = 16,6 \times 10^{10} \, Nm^{-2} \quad ; \quad C_{12} = 7,66 \times 10^{10} \, Nm^{-2} \quad ; \quad C_{13} = 7,75 \times 10^{10} \, Nm^{-2}$$

$$C_{33} = 16,2 \times 10^{10} \, Nm^{-2} \quad ; \quad C_{44} = 4,29 \times 10^{10} \, Nm^{-2}$$

$$e_{15} = 11,6 \, Cm^{-2} \quad ; \quad e_{31} = -4,4 \, Cm^{-2} \quad ; \quad e_{33} = 18,6 \, Cm^{-2}$$

$$k_{11} = 11,16 \times 10^{-9} \, C(Vm)^{-1} \quad ; \quad k_{33} = 12,57 \times 10^{-9} \, C(Vm)^{-1}$$

$$e_D = 4,5 \times 10^{-3} \quad ; \quad P^0 = 0,26 \, Cm^{-2} \quad ; \quad E_C = 2,0 \times 10^5 \, Vm^{-1}$$

REFERENCES

Enderlein, M. (2007), "Finite Elemente Verfahren zur bruchmechanischen Analyse von Rissen in piezoelektrischen Strukturen bei transienter elektromechanischer Belastung", *PhD thesis, TU Bergakademie Freiberg*.

Gross, D. and Seelig, T. (2007), "Bruchmechanik – Mit einer Einführung in die Mikromechanik", 4. Aufl., *Springer-Verlag, Berlin*, 240-252.

Huber, J.E., Fleck N.A., Landis C.M. and McMeeking, R.M. (1999), "A constitutive model for ferroelectric polycrystals", J. Mech. Phys. Solids, **47**, 1663-1697.

Hwang, S.C., Lynch C.S. and McMeeking, R.M. (1994), "Ferroelectric/Ferroelastic interactions and a polarization switching model", Acta metall. mater., **43**(5), 2073-2084.

Jaffe, B., Cook, W.R. and Jaffe, H. (1971), "Piezoelectric ceramics", Academic Press, London.

Kamlah, M. (2000), "Ferroelectric and ferroelastic piezoceramics – modeling of electromechanical hysteresis phenomena", Continuum Mech. Thermodyn., **13**, 219-268.

Kessler, H. and Balke, H. (2001), "On the local and average energy release rate in polarization switching phenomena", J. Mech. Phys. Solids, **49**, 953-978.